MicroRNA-1915-3p prevents the apoptosis of lung cancer cells by downregulating DRG2 and PBX2

CHENGSHAN XU[1*], HENGHENG LI[2*], LING ZHANG[1], TIANJUN JIA[3], LIANNING DUAN[1] and CHENGRONG LU[1]

[1]Aviation Medicine Research Laboratory, Air Force General Hospital, PLA, Beijing 100142;
[2]Graduate Student Ministry of Education; [3]College of Medical Laboratory,
Hebei North University, Zhangjiakou, Hebei 075000, P.R. China

Abstract. Micro (mi)RNAs are short non-coding RNA molecules, which post-transcriptionally regulate gene expression and exert key roles in cell growth, differentiation and apoptosis. In the present study, the mechanism and the function of miR-1915-3p in the apoptotic regulation of lung cancer cell lines (NCI-H441 and NCI-H1650) were investigated. The expression analysis confirmed that the expression of miR-1915-3p was markedly decreased in the apoptotic cells. The overexpression of miR-1915-3p in the lung cancer cells prevented apoptosis induced by etoposide. Developmentally regulated GTP-binding protein 2 (DRG2) and pre-B cell leukemia homeobox 2 (PBX2) were identified as downstream targets of miR-1915-3p, which was shown to bind directly to the 3'-untranslated region of DRG2 and PBX2, subsequently lowering their mRNA and protein expression levels. Co-expression of miR-1915-3p and DRG2/PBX2 in the NCI-H441 and NCI-H1650 cells partly circumvented the effect of miR-1915-3p on apoptosis. The results in the present study revealed that miR-1915-3p functions as a silencer of apoptosis, which regulates lung cancer apoptosis via targeting DRG2/PBX2, and consequently this miRNA may be a putative therapeutic target in lung cancer.

Introduction

Lung cancer is the most commonly diagnosed cancer and leading cause of cancer-associated mortality worldwide, accounting for the mortality of >1 million individuals each year (1-3). Non-small cell lung cancer (NSCLC), including adenocarcinoma and squamous cell carcinoma, is the predominant form of lung cancer, accounting for 75-80% of all cases (4). Previous evidence revealed that miRNAs may be involved in lung cancer, and act as oncogenes or tumor suppressor genes. For example, miR-340 (5), miR-128 (6) and miR-197 (7) were revealed to be deregulated in NSCLC apoptosis. These studies provided novel insights into lung cancer biology, and merited further investigation.

Micro (mi)RNAs are small, non-coding RNAs, 18-23 nucleotides in length, which post-transcriptionally regulate gene expression by base-pairing with target mRNAs in the 3'-untranslated region (UTR) (8). Emerging evidence clearly suggests that the deregulation or dysfunction of miRNAs is associated with crucial biological processes, including development, differentiation, proliferation and apoptosis (9,10). miRNAs function as oncogenes or tumor suppressor genes, depending on the roles of their target genes. Among the miRNAs which are associated with carcinogenesis, miR-1915-3p is one of the most important. The dysregulation of miR-1915-3p was reported in various types of cancer, including prostate cancer (11), renal cell carcinoma (12) and breast cancer (13). miR-1915 regulated the expression of CD133, Paired box gene 2 and Toll-like receptor 2 in adult renal progenitor cells (14). miR-1915 suppressed the expression of B-cell lymphoma (Bcl)-2 at the post-transcriptional level to modulate multidrug resistance by increasing drug sensitivity in human colorectal carcinoma cells (15,16). However, miR-1915-3p remains to be implicated in lung cancer.

In the present study, the role of miR-1915-3p in the etoposide (VP16)-induced apoptosis of lung cancer cells was investigated. miR-1915-3p prevented VP16-induced cell apoptosis, and further investigation revealed that developmentally regulated GTP-binding protein 2 (DRG2) and pre-B cell leukemia homeobox 2 (PBX2) were direct and functional targets of miR-1915-3p. Furthermore, DRG2 and PBX2 may partly circumvent the effect of miR-1915-3p on the apoptosis of H441 and H1650 cells. Therefore, miR-1915-3p is a putative therapeutic agent for the treatment of lung cancer.

Materials and methods

Cell culture. NCI-H441 (H441) and NCI-H1650 (H1650) cells (American Type Culture Collection, Arlington, VA, USA) were maintained in RPMI-1640 medium (Gibco; Thermo

---

Correspondence to: Professor Chengrong Lu, Aviation Medicine Research Laboratory, Air Force General Hospital, PLA, 30 Fucheng Road, Haidian, Beijing 100142, P.R. China
E-mail: luchengrong@263.net

*Contributed equally

Fisher Scientific, Inc., Waltham, MA, USA), supplemented with 10% fetal bovine serum (Beijing Yuanheng Shengma Biotechnology Research Institute, Beijing, China), 100 U/ml streptomycin (Biological Industries, Kibbutz Beit-Haemek, Israel) and 100 U/ml penicillin (Biological Industries), and were maintained at 37˚C in a humidified 5% CO_2 incubator. The medium was changed on alternate days and the cells were split prior to reaching 100% confluence.

Oligonucleotides, plasmids and transfection. An miR-1915-3p mimic (a chemically synthesized, double-stranded miRNA) and miR-1915-3p inhibitor were purchased from GenePharma (Shanghai, China).

The full-length 3'-UTR of DRG2 or PBX2 was subcloned into the pIS0 luciferase plasmid (17) to generate pIS0-DRG2-3'-UTR or pIS0-PBX2-3'-UTR, respectively. Mutant constructs of DRG2 and PBX2-3'-UTR, termed pIS0-DRG2-3'-UTR-mut and pIS0-PBX2-3'-UTR-mut, respecivtely, which bore a replacement of three nucleotides within the core binding sites of DRG2 or PBX2-3-UTR, were synthesized using mutant PCR primers. The primer pairs were as follows: pIS0-DRG2-3'-UTR-forward (F), 5'-TTGAGCTCCCAGCACCAAGTACAGTC-3' and -reverse (R), 5'-GCTCTAGAAAGGAGAGCCAGGAGAAC-3'; pIS0-DRG2-3'-UTR-mut-F, 5'-CCTCGTCTCCAGTGGGAG GTGG-3' and -R, 5'-CCACCTCCCACTGGAGACGAGG-3'; pIS0-PBX2-3'-UTR-F, 5'-TTGAGCTCCGGACGGCTTACT TACCT-3' and -R, 5'-GCTCTAGACTTCACTGCCTCCACA TC-3'; pIS0-PBX2-3'-UTR-mut-F, 5'-GAAAAAGAAACCAGT GGATCCATCT-3' and -R, 5'-AGATGGATCCACTGGTTT CTTTTTC-3'.

The cells were seeded into 6-well plates at $2x10^5$ cells/well. When the cell density reached 60-70%, the cells were transfected with DNA plasmid and oligonucleotide using Lipofectamine 2000 (Invitrogen; Thermo Fisher Scientific, Inc.), according to the manufacturer's instructions.

Prediction of miRNA targets. In order to investigate the predicted target genes, the TargetScan program (http://www.targetscan.org/) and the miRbase program (www.mirbase.org) were used.

RNA extraction and reverse transcription-quantitative polymerase chain reaction (RT-qPCR). The total RNA was extracted using Invitrogen TRIzol reagent (Thermo Fisher Scientific, Inc.). The RT was performed using a FastQuant RT kit [TianGen Biotech (Beijing) Co., Ltd, Beijing, China]. miR-1915-3p was reverse-transcribed using a stem-loop primer (5'-CTCAACTGGTGTCGTGGAGTCGGCAATTCA GTTGAGCCCGCCGC-3'). The RT of DRG2/PBX2 mRNA was performed using a FastQuant RT kit [TianGen Biotech (Beijing) Co., Ltd], according to the manufacturer's protocol. RT-qPCR was performed using a SuperReal PreMix Plus kit [TianGen Biotech (Beijing) Co., Ltd]. U6 small nuclear RNA and β-actin mRNA were used as internal controls for miR-1915-3p and DRG2/PBX2 mRNA, respectively. All reactions were performed in triplicate. The primers used were as follows: DRG2-F, 5'-GCTGAACCTGGACTATCTG-3' and -R, 5'-GAATGATGGCGTCTGTGA-3'; PBX2-F, 5'-CCCATG TCATGAACCTGCTG-3' and -R, 5'-GCGCTGAACTTTCGA TGGAT-3'. The relative fold changes were calculated using the $-2^{\Delta\Delta Cq}$ method, and β-actin was used as an internal control.

Luciferase assay. The cells were cultured in 96-well plates and transiently co-transfected with the miR-1915-3p mimic and the pIS0 vectors using Lipofectamine 2000 reagent (Invitrogen; Thermo Fisher Scientific, Inc.). A scrambled sequence (5'-AACCACUCAACUUUUUCCCAAdTdT-3') was used as a negative control. Following an incubation for 48 h, luciferase activity was measured using a dual luciferase reporter assay system (Promega, Madison, WI, USA). pRL-TK *Renilla* was used as an internal control. Three independent experiments were performed, and all reactions were performed in triplicate.

Flow cytometric analysis (FCM). The cells were seeded into 6-well plates at a density of $5x10^4$ cells/well, and were transfected with the miR-1915-3p mimic or miR-1915-3p inhibitor for 24 h, starved overnight, and treated with etoposide for 48 h. The apoptotic cells were detected using the Annexin V-FITC Apoptosis Detection kit (BD Biosciences, San Jose, CA, USA) and analyzed on a FACSCalibur™ flow cytometer (BD Biosciences) using CellQuest software version 3.3.

Western blotting. The cellular proteins were extracted following treatments, as previously described (18). The protein (20 μg) was loaded into each lane of 8% polyacrylamide gels. The proteins were separated by electrophoresis and the proteins were blotted onto polyvinylidene difluoride membranes (Amersham Pharmacia Biotech, St. Albans, UK) by electrophoretic transfer. The membrane was incubated with primary antibodies goat anti-DRG2 (1:750; cat. no. sc-164233; Santa Cruz Biotechnology, Inc., Santa Cruz, CA, USA), rabbit anti-PBX2 (1:1,000; cat. no. sc-980; Santa Cruz Biotechnology, Inc.) and rabbit anti-β-actin (1:3,000; cat. no. 4970; Cell Signaling Technology, Inc., Beverly, MA, USA), which was used as a loading control.

Statistical analysis. The data are expressed as the mean ± standard deviation from at least three separate experiments, and Student's t-test was performed using SPSS 17.0 software (SPSS, Inc., Chicago, IL, USA). $P < 0.05$ was considered to indicate a statistically significant difference.

Results

miR-1915-3p is involved in lung cancer cell apoptosis. Etoposide (VP16) is known to exert its cancer cell killing effects through induction of apoptosis (19). VP16 induces apoptosis in a number of cancer cell types (20-23), and has been used for the treatment of a wide variety of cancer types (24). In the present study, a marked increase in the levels of apoptosis were detected in H441 and H1650 cells following treatment with VP16 (Fig. 1A and B). RT-qPCR was subsequently performed to assess whether any changes in the level of miR-1915-3p occurred. The expression of miR-1915-3p was markedly downregulated during VP16-induced lung cancer cell apoptosis (Fig. 1C). The reduced expression level of miR-1915-3p during lung cancer apoptosis suggested that this miRNA may exert an antiapoptotic effect. To examine this hypothesis, the effects of transient transfection of the miR-1915-3p mimic, or addition of the miR-1915-3p inhibitor to lung cancer H441 cells, were investigated. Following transfection, the cells were
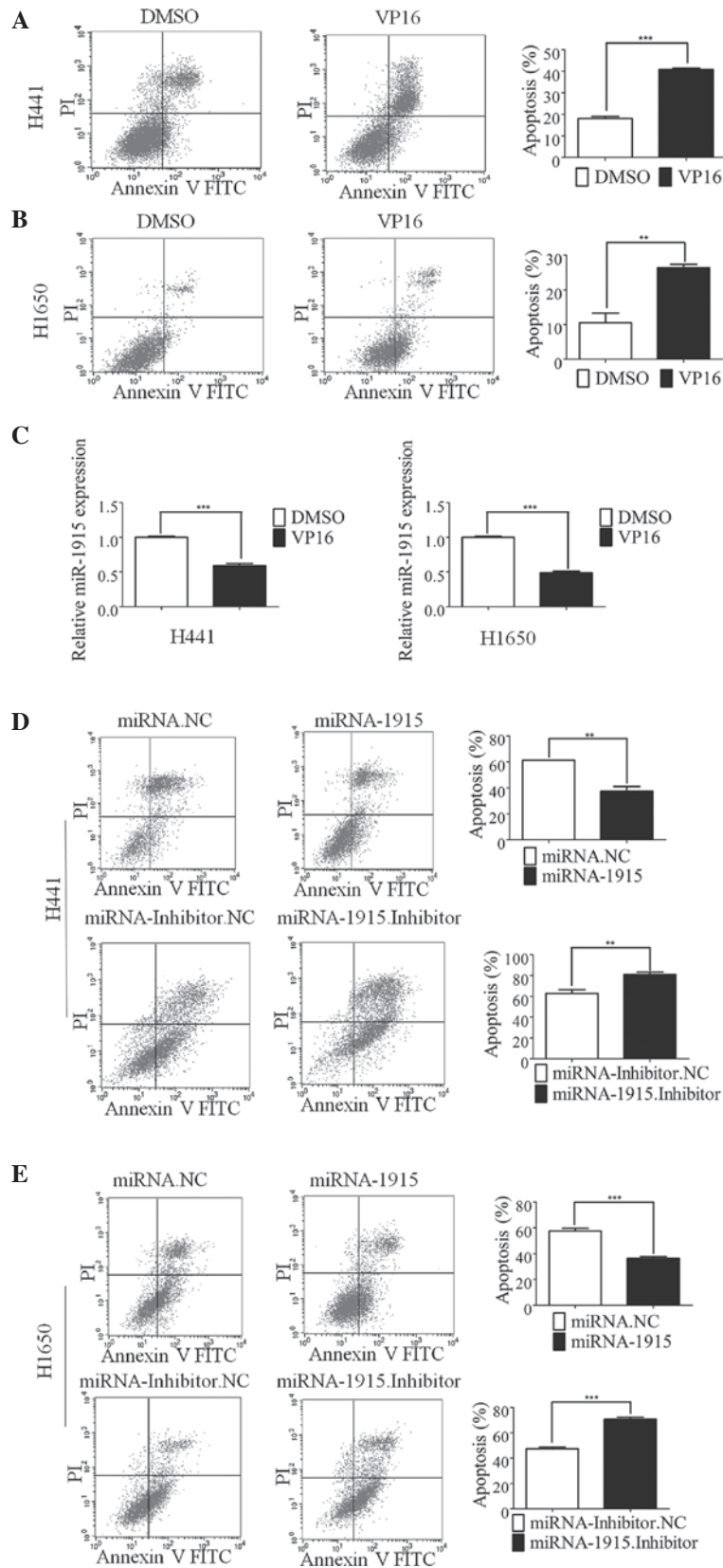
Figure 1. miR-1915 is involved in lung cancer cell apoptosis. (A) The apoptosis of the H441 cells was induced by treatment with 100 μM etoposide (VP16) for 48 h. The histogram shows the percentage of apoptotic cells determined by FCM, and the error bars denote the mean ± standard deviation. (B) The results of FCM are shown, revealing the apoptosis of the H1650 cells following treatment with 100 μM VP16. The histogram shows the percentage of apoptotic cells determined by FCM, and the error bars denote the mean ± standard deviation. (C) The histogram shows the expression of miRNA-1915-3p in the H441 (left) and H1650 cells (right) at 48 h following treatment with 100 μM VP16 treatment. (D) The apoptosis of the H441 cells was induced by treatment with VP16 for 48 h following 24 h transfection with miR-1915-3p mimic. The histogram shows the percentage of apoptotic cells determined by FCM, and the error bars denote the mean ± standard deviation. (E) The apoptosis of H1650 cells induced by treatment with VP16 following miR-1915-3p mimic transfection for 24 h is shown. The histogram shows the percentage of apoptotic cells determined by FCM, and the error bars denote the mean ± standard deviation (**P<0.01 and ***P<0.001, compared with the control, using Student's t-test). DMSO, dimethyl sulfoxide; FCM, flow cytometric analysis; FITC, fluorescein isothiocyanate; miRNA, microRNA; NC, negative control; PI, propidium iodide.
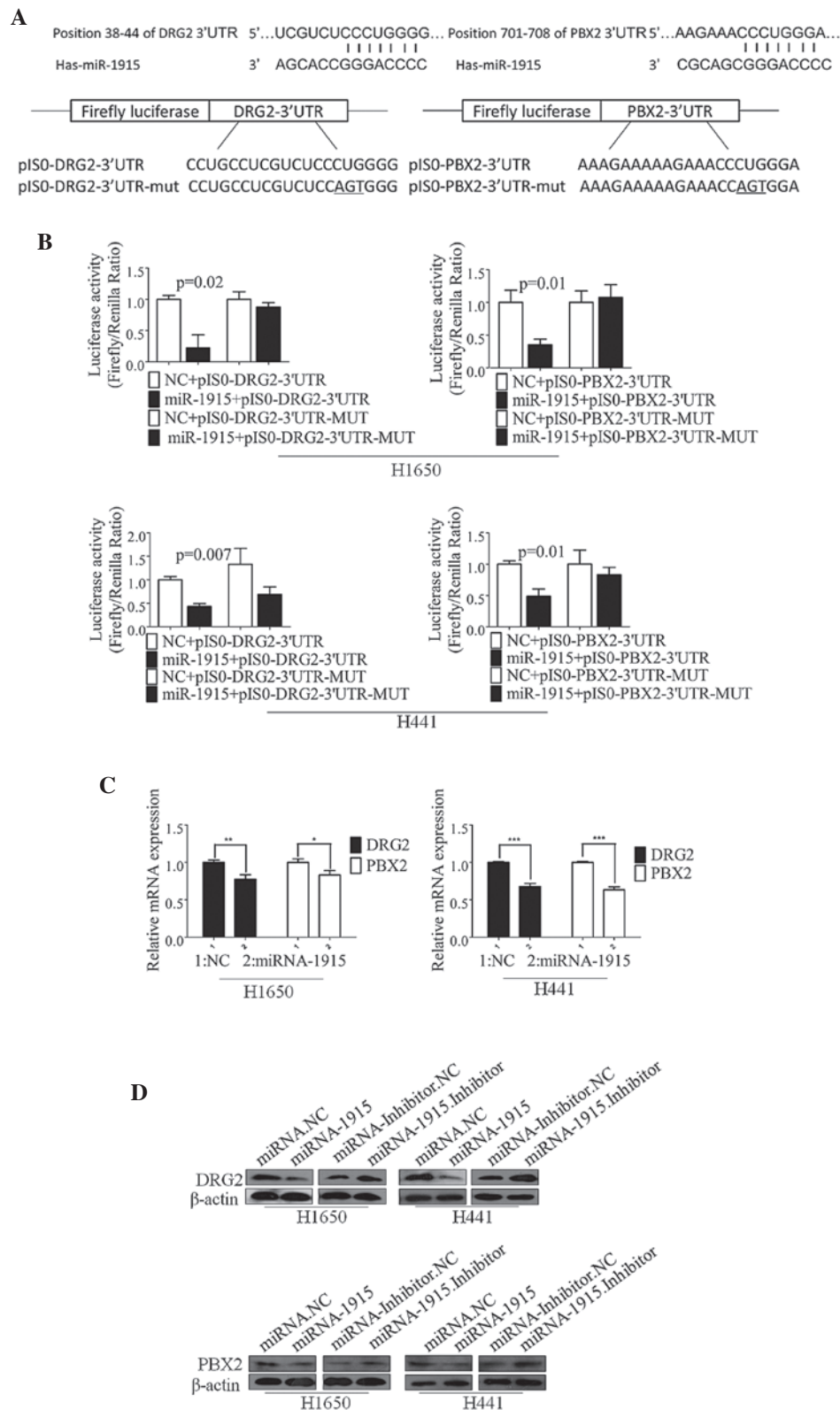
Figure 2. DRG2 and PBX2 are direct targets of miR-1915-3p. (A) The miR-1915-3p targeting site resides at nt 38-44 of the DRG2-3-'UTR and nt 701-708 of the PBX2-3'-UTR. The upper panels are the sequence alignment of miR-1915-3p with binding sites on the DRG2- and PBX2-3'-UTR. The lower panel is a diagram of the luciferase reporter plasmids, including the plasmids with the full-length DRG2-3'-UTR and PBX2-3'-UTR insert (pIS0-DRG2-3'UTR and pIS0-PBX2-3'UTR, respectively) and plasmids with a mutant DRG2-3'-UTR and PBX2-3'-UTR (pIS0-DRG2-3'UTR-MUT and pIS0-PBX2-3'UTR-MUT, respectively), which harbored a replacement of three nts within the miR-1915-3p-binding site. (B) H1650 (upper panels) and H441 (lower panels) cells were transfected with the miR-1915-3p mimic (20 nM) or the plasmids pIS0-DRG2/PBX2-3'-UTR or pIS0-DRG2/PBX2-3'-UTR-mut. pRL-SV40 *Renilla* was used for normalization of the transfection efficiency. Following an incubation for 48 h, the luciferase activities were measured. (C) The expression levels of the DRG2 and PBX2 mRNAs in H1650 (left panel) or H441 (right panel) cell lines, treated as described above, were measured using RT-qPCR. β-Actin was used as internal control. (D) Western blotting was used to detect the expression of DRG2 and PBX2 proteins following transfection of the miRNA-1915-3p mimic (20 nM) or the miRNA-1915-3p inhibitor (40 nM) into the H1650 (left panels) or H441 (right panels) cells. *P<0.05; **P<0.01; ***P<0.001, compared with the NC experiments. DRG2, developmentally regulated GTP-binding protein 2; NC. negative control; nt, nucleotide; PBX2, pre-B cell leukemia homeobox 2; UTR, untranslated region; miRNA, microRNA.
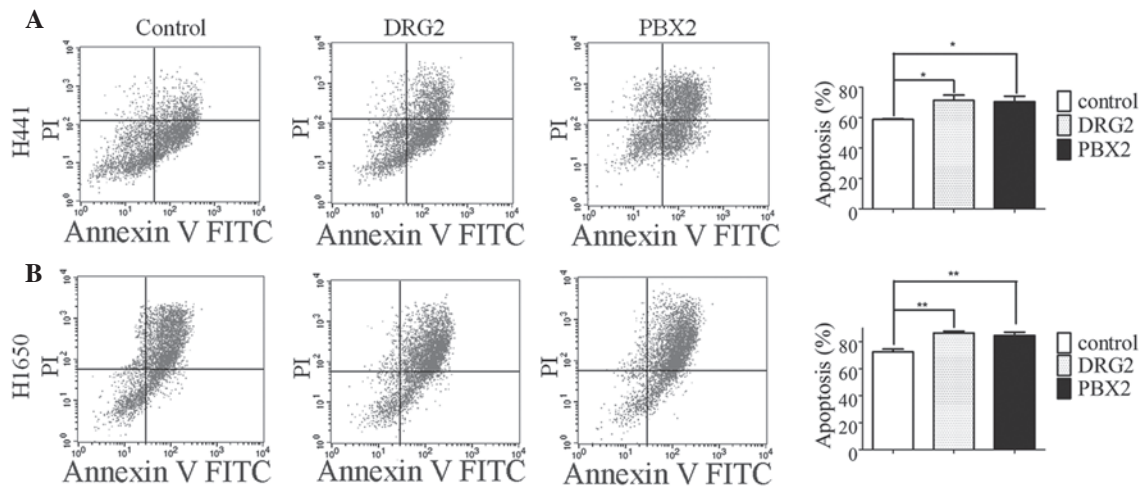
Figure 3. Overexpression of DRG2 or PBX2 promotes VP16-induced cell apoptosis. (A) Apoptosis of the H441 cells was induced by treatment with 100 μM VP16 for 48 h following 24 h transfection with DRG2 or PBX2. The histogram shows the percentage of apoptotic cells determined by FCM, and the error bars denote the mean ± standard deviation. (B) FCM was used to detect apoptosis in the H1650 cells induced by treatment with 100 μM VP16 following DRG2 or PBX2 transfection for 24 h. The histogram shows the percentage of apoptotic cells, and the error bars denote the mean ± standard deviation ([*]P<0.05 and [**]P<0.01, compared with the control). DRG2, developmentally regulated GTP-binding protein 2; FCM, flow cytometric analysis; PBX2, pre-B cell leukemia homeobox 2; FITC, fluorescein isothiocyanate; PI, propidium iodide.

deprived of serum overnight, and were subsequently treated with VP16 for 48 h. FCM was performed to detect the number of apoptotic cells present. Overexpression of the miR-1915-3p mimic markedly inhibited VP16-induced apoptosis (Fig. 1D). By contrast, overexpression of the miR-1915-3p inhibitor elicited the opposite effect, promoting VP16-induced apoptosis (Fig. 1D). A similar phenomenon was also observed in the lung cancer H1650 cells (Fig. 1E). Therefore, these results indicated that miR-1915-3p was associated with lung cancer cell apoptosis.

DRG2 and PBX2 are direct targets of miR-1915-3p. To assess the molecular mechanism of miR-1915-3p in the regulation of apoptosis, putative miR-1915-3p targets were predicted using the target prediction programs, TargetScan, miRanda and miRbase. DRG2 and PBX2 were identified as potential targets of miR-1915-3p. The 3'-UTR of the DRG2 and PBX2 mRNA contained a complementary site for the seed region of miR-1915-3p (Fig. 2A). To determine whether DRG2 and PBX2 were regulated by miR-1915-3p through direct binding to their 3'-UTR sequences, a human DRG2/PBX2 3'-UTR fragment containing wild-type (wt) or mutant miR-1915-3p binding sequence were cloned downstream of the firefly luciferase reporter gene. Co-transfection of the luciferase reporter, pIS0-DRG2/PBX2-3'-UTR-wt and miR-1915-3p, into the lung cancer H1650 cells produced a 50-80% decrease in the luciferase activity compared with the negative control (Fig. 2B). This suppressive effect was rescued by the three nucleotide substitutions (pIS0-DRG2/PBX2-3'UTR-mutant) in the core binding sites, as shown in Fig. 2B (upper panels). A similar effect was identified for the lung cancer H441 cells (Fig. 2B, lower panels).

The effect of miRNA-1915 on the endogenous expression of DRG2/PBX2 was further examined. Marked decreases in the endogenous mRNA (Fig. 2C) and protein (Fig. 2D) expression levels of DRG2 and PBX2 were observed in the H441 and H1650 cells transfected with the miR-1915-3p

mimic, whereas transfection with the miR-1915-3p inhibitor induced a marked increase in the protein expression levels of DRG2/PBX2 (Fig. 2D). These results suggested that miR-1915-3p inhibited the expression of DRG2/PBX2 at the post-transcriptional level by directly targeting the 3'-UTRs of the DRG2/PBX2 mRNA.

Overexpression of DRG2/PBX2 induces apoptosis of the H441 and H1650 lung cancer cells. Since miR-1915-3p decreased the expression of DRG2 and PBX2 and inhibited apoptosis, consequently, the association of DRG2 or PBX with the process of apoptosis in the lung cancer cells was investigated. The H441 cells were transfected with a plasmid harboring DRG2 or PBX2 and deprived of serum overnight, followed by treatment with VP16 for 48 h. FCM was performed to assess the numbers of apoptotic cells. The overexpression of DRG2 or PBX2 significantly promoted VP16-induced apoptosis (Fig. 3A). A similar phenomenon was observed in the H1650 lung cancer cells (Fig. 3B). The identification of DRG2 and PBX2 as novel miR-1915-3p target genes may explain, at least in part, the molecular mechanism of miR-1915-3p.

miRNA-1915 regulates apoptosis through DRG2 and PBX2. Subsequently, whether DRG2 and PBX2 were involved in apoptosis regulated by miRNA-1915-3p was investigated. H1650 cells were co-transfected with the miR-1915-3p mimic and pcDNA3-DRG2 or pcDNA3-PBX2, which encoded the full-length coding region of DRG2/PBX2, although they lacked the 3'-UTR of the DRG2/PBX2 mRNA. The results indicated that overexpression of miR-1915-3p alone decreased the number of VP16-induced apoptotic cells, whereas co-expression with DRG2 or PBX2 effectively reversed the change (Fig. 4A). A similar phenomenon was observed with the H441 cells (Fig. 4B). These results suggested that the apoptotic involvement of miR-1915-3p, at least in part, was dependent on its role in regulating the expression levels of DRG2 and PBX2.
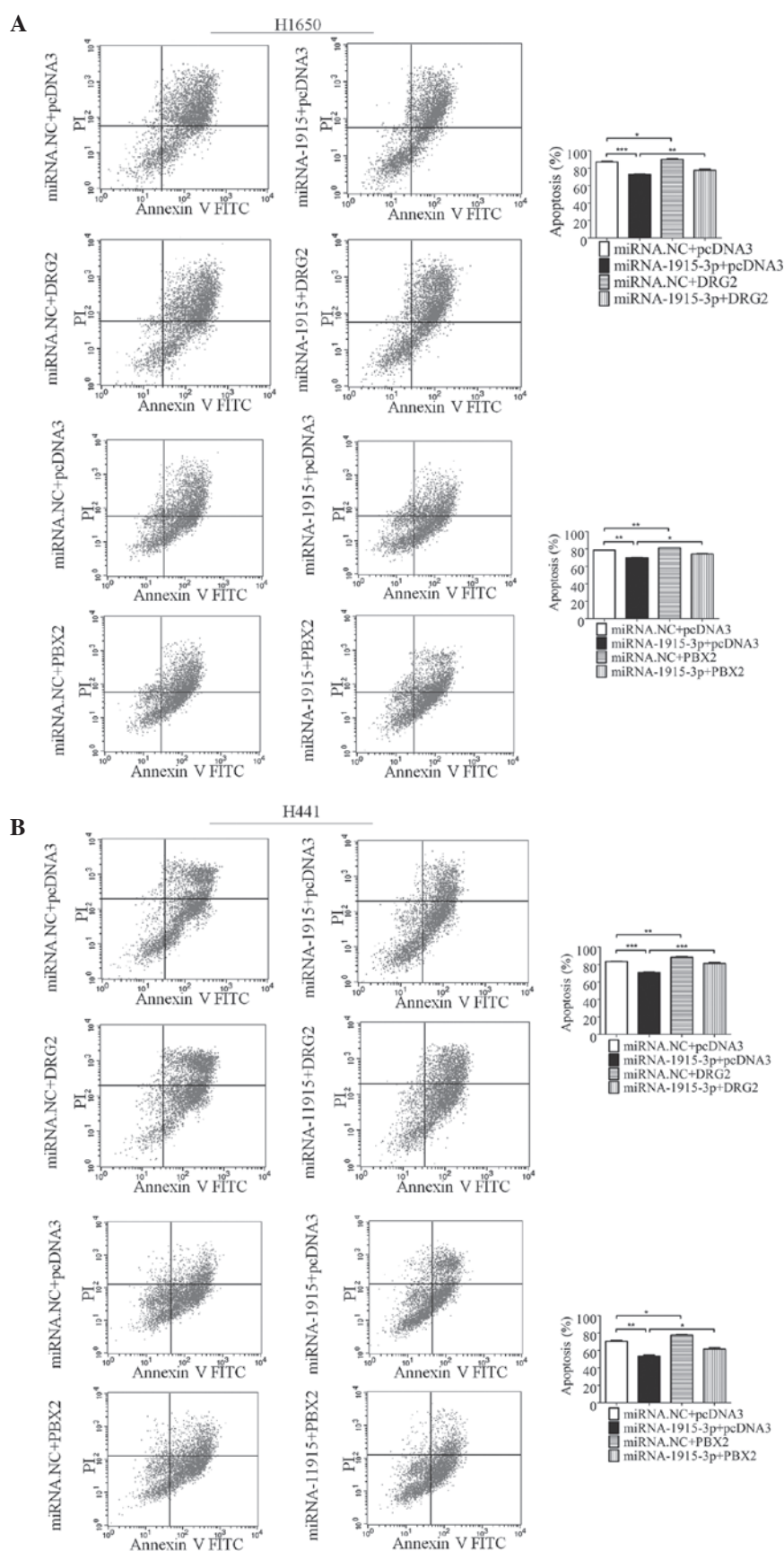
Figure 4. miR-1915-3p regulates apoptosis through DRG2 and PBX2. (A) Apoptosis of the H1650 cells transfected with the miRNA-1915-3p mimic, and/or combined with DRG2 or PBX2 for 48 h was determined using FCM (left). The error bars in the histograms on the right denote the mean ± standard deviation. (B) Apoptosis of the H441 cells at 48 h following transfection of the miRNA-1915-3p mimic, and/or combined with DRG2 or PBX2, was determined by FCM (left). The error bars in the histograms on the right denote the mean ± standard deviation ($^*P<0.05$, $^{**}P<0.01$ and $^{***}P<0.001$, compared with the miRNA. NC+pcDNA3 control, or the miRNA-1915-3p+pcDNA3 experiments). PI, propidium iodide; FITC, fluorescein isothiocyanate; FCM, flow cytometric analysis; DRG2, developmentally regulated GTP-binding protein 2; FCM, flow cytometric analysis; NC, negative control; PBX2, pre-B cell leukemia homeobox 2; miRNA, microRNA.

Discussion

The association of a series of miRNAs with cellular apoptosis has been previously experimentally verified (25-27). In the present study, it was demonstrated that miR-1915-3p was a candidate regulator of lung cancer cell apoptosis. This finding therefore expanded the list of miRNAs which are known to be involved in regulating apoptosis.

The experiments performed in the present study demonstrated that DRG2 and PBX2 were targets of miR-1915-3p. By interacting directly with the 3'-UTRs of the DRG2 and PBX2 mRNA, miR-1915-3p regulated the expression of DRG2 and PBX2 at the post-transcriptional level. The overexpression of miR-1915-3p eliminated VP16-induced apoptosis and led to a marked decrease in the endogenous protein expression of DRG2 and PBX2. DRG2 and PBX2 were therefore associated with apoptosis.

In previously published studies, the overexpression of DRG2 inhibited doxorubicin-induced apoptosis in hepatocellular carcinoma cells (28) and reduced the sensitivity of Jurkat cells to the antimitotic agent, nocodazole (29), although it is unclear whether DRG2 exerts a role in Jurkat cell apoptosis (30). PBX2 is a transcriptional activator, which binds to the T-cell leukemia homeobox protein 1 promoter, and a high level of expression serves as an independent, negative prognostic indicator for gastric cancer and esophageal squamous cell carcinoma (31). However, the roles of DRG2 and PBX2 in lung cancer apoptosis remain to be elucidated. In the present study, it has been demonstrated that the overexpression of DRG2 and PBX2 may markedly promote the VP16-induced apoptosis of lung cancer cells.

In conclusion, the present study demonstrated for the first time, to the best of our knowledge, that the levels of miR-1915-3p are significantly downregulated during the apoptosis of lung cancer cells. The overexpression of miR-1915-3p markedly inhibited VP16-induced cell apoptosis. DRG2 and PBX2 were identified as direct and functional targets of miR-1915-3p. Finally, it was demonstrated that miR-1915 regulates apoptosis via DRG2 and PBX2. These findings may lead to novel therapeutic options for treating human lung cancer.

Acknowledgements

References

1. Siegel R, Ma J, Zou Z and Jemal A: Cancer statistics, 2014. CA Cancer J Clin 64: 9-29, 2014.
2. Ferlay J, Shin HR, Bray F, Forman D, Mathers C and Parkin DM: Estimates of worldwide burden of cancer in 2008: GLOBOCAN 2008. Int J Cancer 127: 2893-2917, 2010.
3. Spiro SG and Silvestri GA: One hundred years of lung cancer. Am. J. Resp. Crit. Care Med 17: 2523-2529, 2005.
4. Harmsma M, Schutte B and Ramaekers FC: Serum markers in small cell lung cancer: Opportunities for improvement. Biochim Biophys Acta 1836: 255-272, 2013.
5. Fernandez S, Risolino M, Mandia N, Talotta F, Soini Y, Incoronato M, Condorelli G, Banfi S and Verde P. miR-340 inhibits tumor cell proliferation and induces apoptosis by targeting multiple negative regulators of p27 in non-small cell lung cancer. Oncogene 34, 3240-3250, 2014.
6. Hu J, Cheng Y, Li Y, Jin Z, Pan Y, Liu G, Fu S, Zhang Y, Feng K and Feng Y: microRNA-128 plays a critical role in human non-small cell lung cancer tumourigenesis, angiogenesis and lymphangiogenesis by directly targeting vascular endothelial growth factor-C. Eur J Cancer 50: 2336-2350, 2014.
7. Fiori ME, Barbini C, Haas TL, Marroncelli N, Patrizii M, Biffoni M and De Maria R: Antitumor effect of miR-197 targeting in p53 wild-type lung cancer. Cell Death Differ 21: 774-782, 2014.
8. Bartel DP: MicroRNAs: Target recognition and regulatory functions. Cell 136: 215-233, 2009.
9. Harfe BD: MicroRNAs in vertebrate development. Curr Opin Genet Dev 15: 410-415, 2005.
10. Bartel DP: MicroRNAs: Genomics, biogenesis, mechanism, and function. Cell 116: 281-297, 2004.
11. He HC, Han ZD, Dai QS, Ling XH, Fu X, Lin ZY, Deng YH, Qin GQ, Cai C, Chen JH, et al: Global analysis of the differentially expressed miRNAs of prostate cancer in Chinese patients. BMC Genomics 14: 757, 2013.
12. White NM, Khella HW, Grigull J, Adzovic S, Youssef YM, Honey RJ, Stewart R, Pace KT, Bjarnason GA, Jewett MA, et al: miRNA profiling in metastatic renal cell carcinoma reveals a tumour-suppressor effect for miR-215. Br J Cancer 105: 1741-1749, 2011.
13. Chen L, Li Y, Fu Y, Peng J, Mo MH, Stamatakos M, Teal CB, Brem RF, Stojadinovic A, Grinkemeyer M, et al: Role of deregulated microRNAs in breast cancer progression using FFPE tissue. PLoS One 8: e54213, 2013.
14. Sallustio F, Serino G, Costantino V, Curci C, Cox SN, De Palma G and Schena FP: miR-1915 and miR-1225-5p regulate the expression of CD133, PAX2 and TLR2 in adult renal progenitor cells. PLoS One 8: e68296, 2013.
15. Nakazawa K, Dashzeveg N and Yoshida K: Tumor suppressor p53 induces miR-1915 processing to inhibit Bcl-2 in the apoptotic response to DNA damage. FEBS J 281: 2937-2944, 2014.
16. Xu K, Liang X, Cui D, Wu Y, Shi W and Liu J: miR-1915 inhibits Bcl-2 to modulate multidrug resistance by increasing drug-sensitivity in human colorectal carcinoma cells. Mol Carcinog 52: 70-78, 2013.
17. Yekta S, Shih IH and Bartel DP: MicroRNA-directed cleavage of HOXB8 mRNA. Science 304: 594-596, 2004.
18. Dong Y, Xiong M, Duan L, Liu Z, Niu T, Luo Y, Wu X, Xu C and Lu C: H2AX phosphorylation regulated by p38 is involved in Bim expression and apoptosis in chronic myelogenous leukemia cells induced by imatinib. Apoptosis 19: 1281-1292, 2014.
19. Pommier Y, Leo E, Zhang H and Marchand C: DNA topoisomerases and their poisoning by anticancer and antibacterial drugs. Chem Biol 17: 421-433, 2010.
20. Cui X, Choi HK, Choi YS, Park SY, Sung GJ, Lee YH, Lee J, Jun WJ, Kim K, Choi KC, et al: DNAJB1 destabilizes PDCD5 to suppress p53-mediated apoptosis. Cancer Lett 357: 307-315, 2015.
21. Park JH, Lee SW, Yang SW, Yoo HM, Park JM, Seong MW, Ka SH, Oh KH, Jeon YJ and Chung CH: Modification of DBC1 by SUMO2/3 is crucial for p53-mediated apoptosis in response to DNA damage. Nat Commun 5: 5483, 2014.
22. Okamoto S, Jiang Y, Kawamura K, Shingyoji M, Tada Y, Sekine I, Takiguchi Y, Tatsumi K, Kobayashi H, Shimada H, et al: Zoledronic acid induces apoptosis and S-phase arrest in mesothelioma through inhibiting Rab family proteins and topoisomerase II actions. Cell Death Dis 5: e1517, 2014.
23. Liu J, Uematsu H, Tsuchida N and Ikeda MA: Essential role of caspase-8 in p53/p73-dependent apoptosis induced by etoposide in head and neck carcinoma cells. Mol Cancer 10: 95, 2011.
24. Hande KR: Etoposide: Four decades of development of a topoisomerase II inhibitor. Eur J Cancer 34: 1514-1521, 1998.
25. Zhang Y, Geng L, Talmon G and Wang J: MicroRNA-520g confers drug resistance by regulating p21 expression in colorectal cancer. J Biol Chem 290: 6215-6225, 2015.
26. Adi Harel S, Bossel Ben-Moshe N, Aylon Y, Bublik DR, Moskovits N, Toperoff G, Azaiza D, Biagoni F, Fuchs G, Wilder S, et al: Reactivation of epigenetically silenced miR-512 and miR-373 sensitizes lung cancer cells to cisplatin and restricts tumor growth. Cell Death Differ 22: 1328-1340, 2015.
27. Yang CH, Pfeffer SR, Sims M, Yue J, Wang Y, Linga VG, Paulus E, Davidoff AM and Pfeffer LM: The oncogenic microRNA-21 inhibits the tumor suppressive activity of FBXO11 to promote tumorigenesis. J Biol Chem 290: 6037-6046, 2015.

28. Chen J, Shen BY, Deng XX, Zhan Q and Peng CH: SKP1-CULLIN1-F-box (SCF)-mediated DRG2 degradation facilitated chemotherapeutic drugs induced apoptosis in hepatocellular carcinoma cells. Biochem Biophys Res Commun 420: 651-655, 2012.
29. Song H, Kim SI, Ko MS, Kim HJ, Heo JC, Lee HJ, Lee HS, Han IS, Kwack K and Park JW: Overexpression of DRG2 increases G2/M phase cells and decreases sensitivity to nocodazole-induced apoptosis. J Biochem 135: 331-335, 2004.
30. Ko MS, Lee UH, Kim SI, Kim HJ, Park JJ, Cha SJ, Kim SB, Song H, Chung DK, Han IS, *et al*: Overexpression of DRG2 suppresses the growth of Jurkat T cells but does not induce apoptosis. Arch Biochem Biophys 422: 137-144, 2004.
31. Qiu Y, Song B, Zhao G, Deng B, Makino T, Tomita Y, Wang J, Luo W, Doki Y, Aozasa K, *et al*: Expression level of Pre B cell leukemia homeobox 2 correlates with poor prognosis of gastric adenocarcinoma and esophageal squamous cell carcinoma. Int J Oncol 36: 651-663, 2010.